Spatiotemporal evolution of continuous-wave field and dark soliton formation in a microcavity with normal dispersion*

Xiaohong Hu(胡晓鸿)[1,2,3], Wei Zhang(张伟)[1], Yuanshan Liu(刘元山)[1], Ye Feng(冯野)[1], Wenfu Zhang(张文富)[1], Leiran Wang(王擂然)[1], Yishan Wang(王屹山)[1,3,†], and Wei Zhao(赵卫)[1,3]

[1] *State Key Laboratory of Transient Optics and Photonics, Xi'an Institute of Optics and Precision Mechanics, Chinese Academy of Sciences, Xi'an* 710119, *China*

[2] *University of Chinese Academy of Sciences, Beijing* 100049, *China*

[3] *Collaborative Innovation Center of Extreme Optics, Shanxi University, Taiyuan* 030006, *China*

(Received 20 January 2017; revised manuscript received 15 March 2017; published online 6 June 2017)

Stable dark soliton and dark pulse formation in normally dispersive and red-detuned microcavities are investigated by numerically solving the normalized Lugiato-Lefever equation. The soliton essence is proved by fitting the calculated field intensity profile with the analytical formula of a dark soliton. Meanwhile, we find that a dark soliton can be generated either from the nonlinear evolution of an optical shock wave or narrowing of a locally broad dark pulse with smoother fronts. Explicit analytical expression is obtained to describe the oscillatory fronts of the optical shock wave. Furthermore, from the calculation results, we show that for smaller frequency detunings, e.g., $\alpha < 3$, in addition to the dark soliton formation, a single dark pulse with an oscillatory dip can also arise and propagate stably in the microcavity under proper pump detuning and pump strength combination. The existence region together with various field intensity profiles and the corresponding spectra of single dark pulse are demonstrated.

Keywords: pulse propagation, temporal solitons, microcavities, nonlinear optics

PACS: 42.65.Tg, 42.65.–k, 42.65.Wi **DOI:** 10.1088/1674-1056/26/7/074216

1. Introduction

Kerr optical frequency combs generation via the parametric four-wave mixing (FWM) processes in microcavities have attracted a great deal of attention and been studied widely.[1,2] Various kinds of microcavity structures and materials have been designed and adopted, such as the doped silica glass ring resonator,[3] silica microtoroid,[4] aluminum nitride (AlN) and silicon nitride (Si_3N_4) microring resonators,[5–7] crystalline CaF_2 and MgF_2 microtoroids.[8,9] In the early stage of research, spectral properties of the optical frequency combs, including the wavelength range and spectral bandwidth received more attention. Near-infrared frequency combs, in which the pump wavelength located in the communication band, e.g. around 1550 nm, were firstly reported in Refs. [10] and [11]. Optical frequency combs in the mid-infrared and visible wavelength range were also obtained successively by adopting different microresonator structures and pump sources.[12–17] In these cases, the microcavities showed an anomalous dispersion at the pump wavelength and therefore the positive nonlinear phase mismatch could be compensated by the anomalous dispersion. Due to the modulation instability (MI) effect, two sidebands corresponding to the maximum parametric gain arise from the intensity fluctuations of the pump field, which usually results in the formation of the so-called primary comb teeth. In most cases, the separation between the newly generated sidebands and the pump mode is equal to multiple free-spectral range (FSR) of the adopted microcavity. In the process, the energy conservative law is conserved. Explicitly, the energy of two pump photons are converted into the pairwise equidistant sidebands. The pump mode and the generated sidebands then further serve as the new pump photons and act together to excite two other comb modes through the cascaded or nondegenerate FWM processes.[2] In FWM combs , the phases of the comb modes are determined by the generation process, which keeps constant but random. This leads to a periodic but not pulsed intracavity waveform.[18] Phase synchronization or mode locking of all the comb teeth, which result in the formation of dissipative bright solitons, can be realized by carefully tuning the frequency difference between the pump laser and the cavity resonance. The microcavity is red detuned and the comb spectrum exhibits a smooth and triangular profile. It is worth noting that all the comb modes contribute to the shaping of the bright soliton pulse. Meanwhile, the available minimum soliton width is determined by the cavity parameters, such as group-velocity dispersion (GVD), effective nonlinearity and loaded quality factor.[18]

In parallel with the study of parametric processes in a microcavity with anomalous dispersion, Kerr optical frequency combs formation in the normal dispersion region are also investigated both theoretically and experimentally. For one

*Project supported by the National Key Research and Development Program of China (Grant No. 2016YFF0200702), the National Natural Science Foundation of China (Grant Nos. 61690222 and 11573058), and the CAS-SAFEA International Partnership Program for Creative Research Teams.

†Corresponding author. E-mail: yshwang@opt.ac.cn

© 2017 Chinese Physical Society and IOP Publishing Ltd

thing, resulting from the additional degree of freedom, namely frequency detuning of the pump laser from the cavity resonance, MI can also take place in normally dispersive microcavities. However, the investigation results reveal that the generation of a Kerr optical frequency comb from noise by using MI is only possible for large frequency detuning cases. Only in this situation, the parametric gain spectrum of the first sidebands is separated from that of the continuous-wave (CW) instability by a sizable window. Accordingly, MI is able to act under a sufficient long time for the microcavity system to end up in a comb state.[19] For another thing, optical frequency combs generated in a normally dispersive microcavity can be attributed to the formation of dark soliton or pulses in most cases. A fundamental optical frequency comb including approximately 80 harmonics was demonstrated in a MgF_2 whispering-gallery mode microresonator with normal dispersion, 9.9-GHz FSR and a quality factor exceeding 2.5×10^9.[20] Unlike the smooth and triangular comb profile of a bright soliton pulse, the generated comb spectrum exhibited some symmetric peak-like or shoulder structures. The phase locking state and formation of dark pulses inside the microresonator were further probed by numerically solving the equations describing the behavior of 101 comb modes. In a recent experiment, a Si_3N_4 microring with a large normal dispersion and loaded quality factor of 7.7×10^5 was adopted to investigate the formation of mode-locked dark pulses and the related Kerr comb structures.[21] The time-domain waveform in the microcavity was reconstructed by using the spectral phase information retrieved via line-by-line pulse shaping and the measured power spectrum. The existence of square dark pulses with chirped edges and ripples at the pulse bottom was further verified from the reconstructed waveform.

In this article, nonlinear evolutions of a CW field in red-detuned microcavities with normal dispersion are investigated by numerically solving the normalized Lugiato-Lefever equation (LLE). The formation of a stable dark soliton, multiple dark solitons or a single dark pulse in the pump detuning region of $\alpha < 3$ are probed by adding an additional white Gaussian noise to the initial CW field. Local generation of an optical shock wave with oscillatory fronts or a locally broad dark pulse with wide bottom are identified to represent different routes to a dark soliton. In order to verify the soliton essence, a modified analytical expression based on the general solution of a dark soliton is adopted to fit the numerically obtained field intensity profile. Furthermore, an explicit analytical expression is derived to describe the oscillatory fronts of the optical shock wave. Finally, we present the existence region together with various single dark-pulse-related field and spectral profiles corresponding to different combinations of cavity detuning and external pump parameter.

2. Theoretical model

The normalized LLE defined by Eq. (1) describes a nonlinear system with damping, detuning and driving, which can be used to study the field evolution and optical Kerr frequency comb generation in a microresonator[22–25]

$$\frac{\partial\psi}{\partial\tau} = -(1+\mathrm{i}\alpha)\,\psi + \mathrm{i}\,|\psi|^2\,\psi - \mathrm{i}\frac{\beta}{2}\frac{\partial^2\psi}{\partial\theta^2} + F, \tag{1}$$

where $\psi(\tau,\theta) = (2g_0/\Delta w_{l0})^{1/2}A^*$ is the rescaled slowly varying envelope of the total intracavity field A. The dimensionless parameter $\tau = t/2\tau_{\mathrm{ph}}$ is the rescaled propagation time used to describe the evolution of intracavity field over successive round-trips and τ_{ph} denotes the photon lifetime. θ represents the azimuthal angle along the circumference of the microresonator. The parameter $g_0 = n_2 c h w_{l0}^2/(n_0^2 V_0)$ denotes the parametric gain of the FWM process in a microcavity where n_0 and n_2 are the linear and nonlinear refraction indices of the bulk material, respectively, h is Planck's constant and V_0 is the effective mode volume of the pump laser. $\alpha = -2(\Omega_0 - w_{l0})/\Delta w_{l0}$ represents the rescaled cavity detuning parameter relative to half mode linewidth where Ω_0 and w_{l0} are the frequencies of pump laser and the corresponding cavity resonance mode. The second item on the right-hand side of Eq. (1) describes the field intensity dependent nonlinear Kerr effect. The second-order dispersion is described by the parameter $\beta = 2c/n_0(2\pi FSR)^2\beta_2/\Delta w_{l0}$, in which parameters c, β_2, and Δw_{l0} represent the vacuum speed of light, GVD, and linewidth of the pump mode, respectively. The driving parameter F is related to the real pump power P through Eq. (2)[26]

$$F = \sqrt{\frac{8g_0\Delta w_{\mathrm{ext}}}{\Delta w_{\mathrm{tot}}^3}\frac{P}{\hbar\Omega_0}}, \tag{2}$$

where the parameters Δw_{ext} and Δw_{tot} represent the coupling and total linewidths at the pump frequency. In addition, for the fundamental TE-polarized mode,[27] the cavity resonance frequency w_{l0} can be derived by using an asymptotic expansion.[28]

We solve the LLE by using the standard split-step Fourier method.[29] Considering the periodical characteristic of the field propagating in a microcavity, we adopt the fast Fourier transform (FFT) algorithm in this method to implement the Fourier-transform operation and greatly shorten the calculation time.

3. Dark soliton formation

In order to probe the availability of pulsed field profiles and their corresponding comb spectra in a microcavity with normal dispersion, an additional white Gaussian noise is added to the initial CW field. The amplitude signal-to-noise ratio (SNR) between the CW field and the noise background is set to be 30 dB. The calculation results shown in Fig. 1 indicate

that some stable dark solitons can form in the cavity. In the situation of single dark soliton generation, the frequency comb exhibits a smooth and triangular profile with the mode spacing equal to one FSR. In addition to the pulsed field profile, the initial CW field in the time domain evolves to the uppermost homogeneous steady state (HSS) with an intensity ρ determined by the cavity detuning α and pump parameter F. An analytical expression based on the general solution of dark soliton[26] is given by

$$I_s^2(\theta) = \eta^2 \left\{1 - B^2 \mathrm{sech}^2\left[\tau_s(\theta - \theta_s)\right]\right\}, \tag{3}$$

where the parameters η and θ_s represent the soliton amplitude and the soliton dip location. Physically, B governs the depth of the dip ($|B| \leq 1$). Different from the case of fiber dark soliton pulse,[29,30] an additional parameter τ_s relating to the width of a dark soliton is required. We adopt Eq. (3) to fit the numerically obtained field profile, and results are shown in Fig. 1(a) The obtained fitting parameters are $\eta = 1.604$, $B = 0.848$, $\tau_s = 4.52$, and $\theta_0 = 0.02$. The good match between the analytical solution and the numerically obtained field profile indicates that the generated dark pulses in the microcavity are stable dissipative dark solitons.

Meanwhile, as shown in Figs. 1(d) and 1(f), more complex frequency comb spectra with mode-to-mode intensity fluctuation are observed when multiple dark solitons coexist in the microcavity. The deviation of the pulse separation from a 2π/N angle is responsible for the intensity modulation of the comb spectrum.[26]

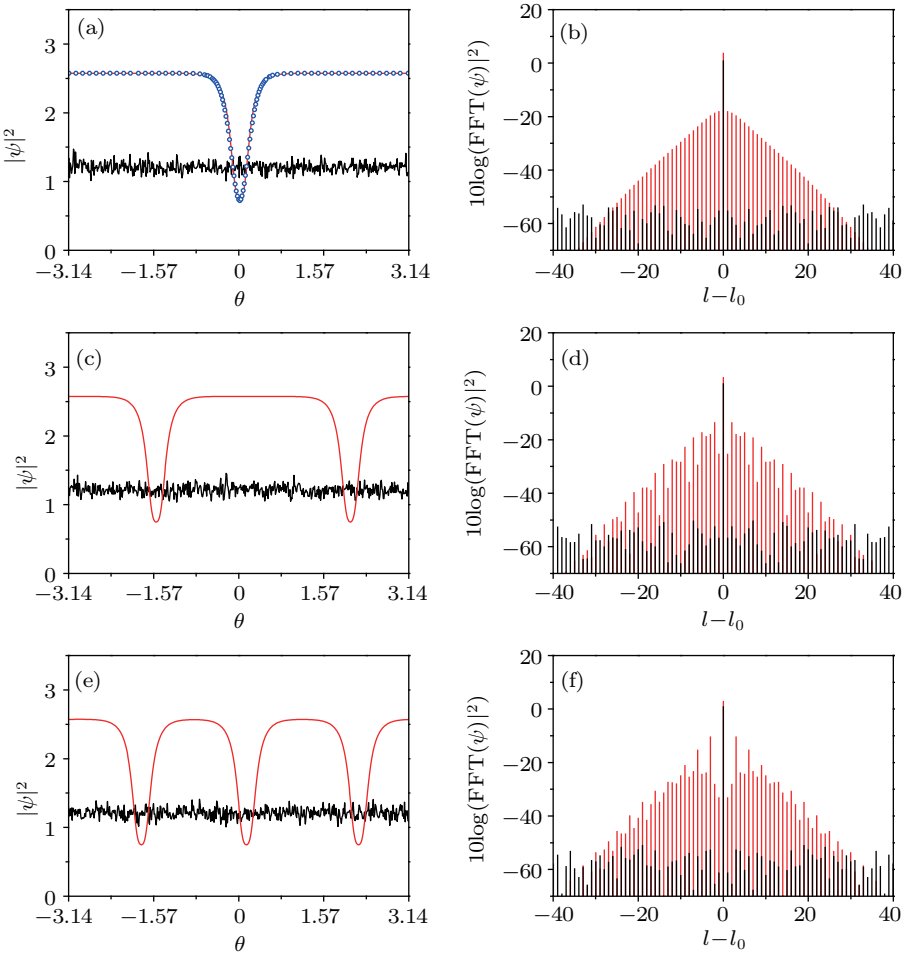


Fig. 1. (color online) Dark soliton forms from the nonlinear evolution of an initial steady-state CW field with white Gaussian noise. The left column shows the initial (black) and ultimate (red) formed field profiles. The right column gives the corresponding spectral profiles. An analytical fitting of the numerically obtained field intensity profile based on Eq. (3) is exhibited as the blue circles in (a). The cavity and pump parameters adopted during the calculation process are: $\alpha = 2.5$, $\beta = 0.0125$, $F = 1.61$, $\rho = 1.209$.

A nonlinear system with bistability can provide the most convenient operating regime for observing optical shock waves, nonstationary fast wavetrains that develop owing to the regularizing action of weak dispersion over steep wave fronts forming via a gradient catastrophe.[30] We find that the formation of a stable dark soliton from a CW field with white Gaussian noise mainly includes two physical processes: one is the generation of optical shock wave with oscillatory fronts and the other is the motion and interlocking of the oscillatory wave fronts. As shown in Fig. 2, in the early stage of the evolution, the weak normal dispersion concurs with the nonlinear Kerr effect to drive the steepening of the pulse edge. Once an

optical shock wave is formed, the successive circulation in the microcavity is dominated by the traveling of the optical shock wave with nearly invariant fronts. Eventually, the formation of a localized and stable dissipative dark soliton terminates the further broadening of the shock wave.

We further observe that the bottom $\rho_{\rm down}$ and flat top $\rho_{\rm up}$ intensities of the shock waves are equal to those of the HSSs. They are determined by the frequency detuning α and external pump F parameters through the functional relation $F^2=\rho[1+(\rho-\alpha)^2]$. Taking the selected parameters $\alpha=2.5$ and $F=1.61$ for example, the calculated field intensities of the stable HSSs are $\rho_{\rm down}=0.53$ and $\rho_{\rm up}=2.57$. The numerical values in Fig. 3(a) accord well with the theoretical ones. Therefore, the oscillatory fronts of the formed optical shock wave actually connect the upper and lower HSSs of the bistable microcavity system. Resulting from the wide pulse width of the optical shock wave, the bandwidth of the frequency comb is narrower than that of a dark soliton.

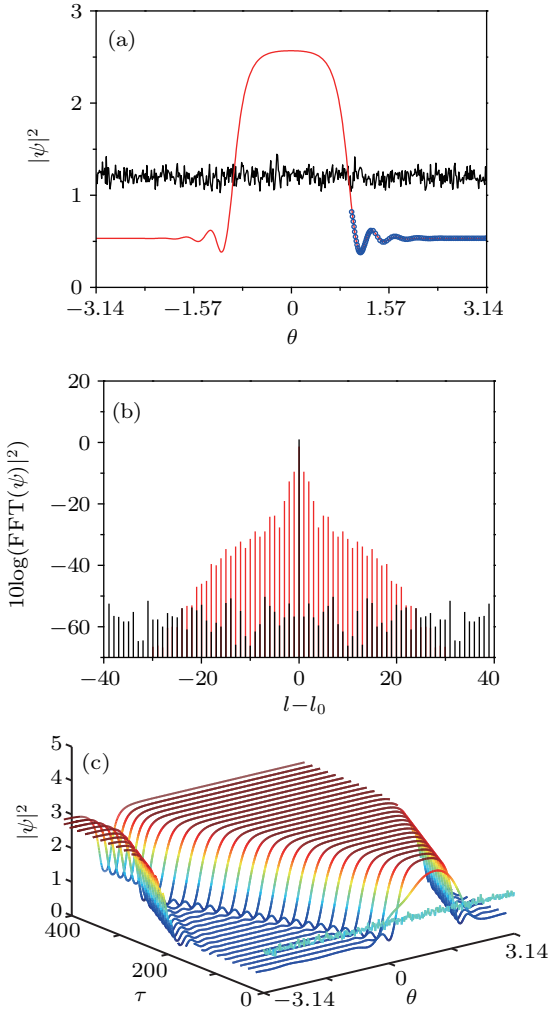


Fig. 2. (color online) Optical shock wave forms and evolves towards a stable dark soliton. (a) Profiles of the initial CW field (black) with white Gaussian noise and the formed optical shock wave (red). An analytical fitting of the oscillatory wave front based on Eq. (4b) is also shown as the blue circles. (b) The corresponding comb spectra. (c) Field evolution pattern. The parameters adopted in the process of calculation are: $\alpha=2.5$, $\beta=0.0125$, $F=1.61$, $\rho=1.2$.

The investigations further suggest that the oscillatory structure of the wave fronts may be approximated in the form $\psi(\theta)-\psi_{\rm down}(\theta)\propto \mathrm{e}^{\lambda\theta}$ where $\psi(\theta)$ represents the complex amplitude of the wave front.[31] The parameter $\lambda=q+\mathrm{i}w$ is a complex eigenvalue in which q and w determine the damping rate and frequency of the oscillation, respectively. In order to obtain an analytical expression which can be used to describe the oscillatory structure in the wave fronts, we further introduce a complex constant C and the complex amplitude has a form of $\psi(\theta)=\psi_{\rm down}(\theta)+C\mathrm{e}^{\lambda\theta}$. The analytical expressions of the oscillations in the wave fronts are derived as follows:

$$\psi(\theta) = |\psi_{\rm down}|\,\mathrm{e}^{\mathrm{i}\phi_{\rm down}}+|C|\,\mathrm{e}^{q(\theta-\theta_0)}\,\mathrm{e}^{\mathrm{i}[w(\theta-\theta_0)+\phi_{\rm c}]}, \quad (4a)$$

$$|\psi(\theta)|^2 = \psi(\theta)\cdot\psi^*(\theta)=\rho_{\rm down}+|C|^2\,\mathrm{e}^{2q(\theta-\theta_0)} +2|\psi_{\rm down}||C|\,\mathrm{e}^{q(\theta-\theta_0)}\cos[w(\theta-\theta_0)+\phi_0], \quad (4b)$$

where the parameter $\rho_{\rm down}=|\psi_{\rm down}|^2$ denotes the field intensity of the lower HSS and the constant phase factor $\phi_0=\phi_{\rm c}-\phi_{\rm down}$ is the phase difference between the complex constant C and lower HSS $\psi_{\rm down}$. The parameter θ_0 determines the position of the oscillation along the azimuthal direction. For the specific case shown in Fig. 3, the obtained fitting parameters are $q=-3.72$, $w=17.01$, $|C|=0.89$, $\theta_0=0.57$, and $\phi_0=0.01$. The good fitting result proves the effectiveness and validity of Eq. (4) to describe the oscillatory structures of the wave fronts.

The difference of the profile similarity between the optical shock wave and the flat-top dissipative solitonic pulses or "platicons" is considered. Stable platicons can be generated in a microcavity with normal GVD when large and positive eigenfrequency shift of the pumped mode is obtained.[32] This can be realized through the mode coupling process or by using a strong self-injection locking technique. Different from the situation in Ref. [32], we assume in our model the frequency of the pumped mode is unperturbed and thus no eigenfrequency shifting occurs in the field evolution process. Therefore, the evolution pattern shown in Fig. 2(c) reveals that the formed optical shock wave is not a stable cavity state and eventually evolves into a dark soliton.

The existence of dark soliton in the region where MI is absent ($\alpha<2$) is investigated as well. The ultimate stable field and comb spectral profile together with the evolution pattern are shown in Fig. 3. Different from the formation process described in Fig. 2, a wide and dark pulse with flat bottom arises firstly. The subsequent evolution process involves the narrowing of the pulse bottom and the formation of a stable dark soliton. For a smaller frequency detuning, close to the lower HSS, though symmetrical intensity fluctuations of the wave fronts which connect the upper and lower HSSs are also observed with the successive evolution of the broad dark pulse in the cavity, the oscillations become much weaker and

smoother compared with the situation shown in Fig. 2. Meanwhile, because of the reduced bistable region, the generation of a stable dark soliton in this region imposes a strict requirement on the pump parameter, as shown in Fig. 4.

$$F^2 = 1 + (1-\alpha)^2, \tag{5a}$$

$$F^2 = \frac{2\alpha + \sqrt{\alpha^2 - 3}}{3}\left[1 + \left(\frac{\alpha - \sqrt{\alpha^2 - 3}}{3}\right)^2\right]. \tag{5b}$$

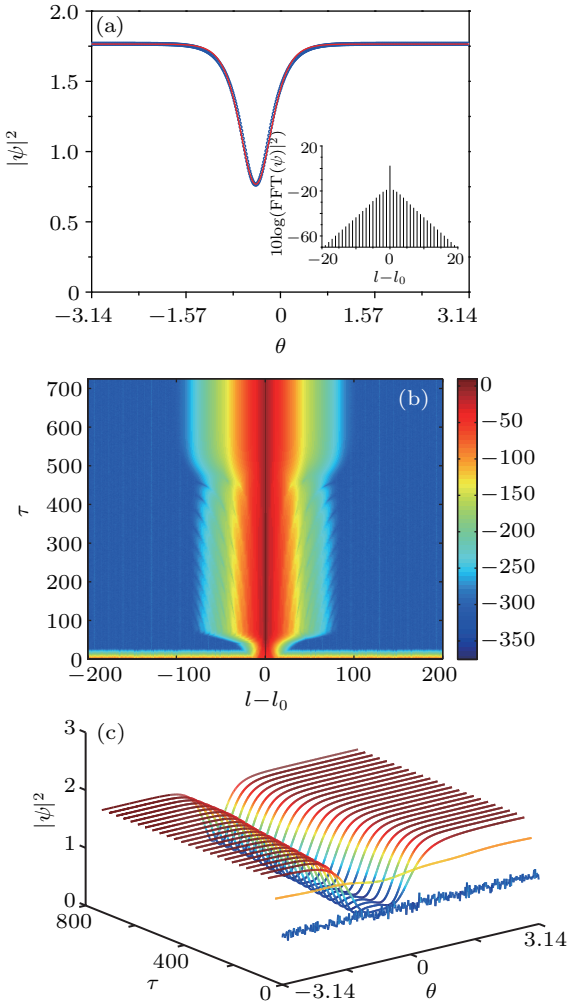


Fig. 3. (color online) Dark soliton formation in the region of $\alpha < 2$. (a) Soliton intensity profile. Fitting of the field profile based on Eq. (3) is shown by the blue circles and the inset gives the corresponding comb spectrum. (b) Evolution pattern of spectral intensity represented as a color density plot. (c) Field evolution pattern. The parameters adopted in the process of calculation are: $\alpha = 1.95$, $\beta = 0.0125$, $F = 1.353$, $\rho = 0.853$.

For the studied frequency detuning region of $\alpha < 3$, figure 4 gives the existence region of a single dark-pulse-related field profile in the (α, F) parameter space. Although the existence region was also provided in Ref. [26], only the field intensity profile of a dark soliton was found and discussed in the case of $\alpha < 3$. By adopting a different initial condition, e.g., a CW wave with white Gaussian noise, we further observe that a single dark pulse with an oscillatory dip can also arise and propagate stably in the microcavity under proper pump detuning and pump strength combinations, with $\alpha = 2.5$ and $F = 1.5965$. In addition, the inset exhibits the calculated dark soliton and dark pulse-related field intensity and spectral profiles at certain (α, F) combinations. As shown in Fig. 4, a larger frequency detuning corresponds to a wider existence region of single dark pulse and looser requirement on the pump intensity. Meanwhile, a wider spectral bandwidth is related to a larger frequency detuning and a higher pump intensity. When an oscillatory structure is present at the bottom of the formed dark pulse, the spectral profile deviates from the smooth edged triangular shape of a dark soliton and instead exhibits a shoulder-like structure. We note that similar spectral profiles can be formed from different (α, F) combinations, e.g. cases of $\alpha = 2.5$, $F = 1.59648$ and $\alpha = 2.9$, $F = 1.761$. The finite multiplicity of dark pulses originates from a collapsed snaking structure of the bifurcation at the upper saddle node. For a given frequency detuning, when the pump parameter F is close to the Maxwell point, a temporally broad dark pulse can form in the microcavity.[31,33]

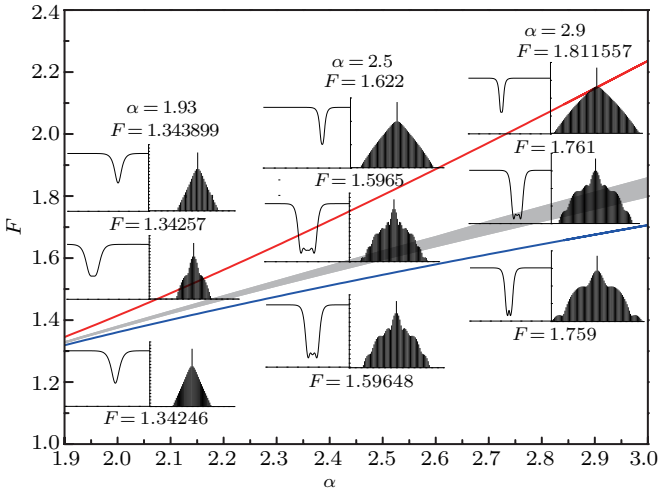


Fig. 4. (color online) Existence region of a single dark pulse (gray) in the (α, F) parameter space. The inset exhibits some typical, single dark-pulse-related field intensity profiles and their comb spectra. The blue and red curves determine the pump boundaries of dark pulse generation. For the two curves, the functional relation between F^2 and α is given by Eq. (5).

4. Conclusion

Dark solitons, dark-pulse-related field profiles, and their corresponding comb spectra are obtained by numerically propagating CW fields with white Gaussian noise in normally dispersive microcavities. We find that, in the frequency detuning region of $\alpha < 3$, for proper frequency detuning and pump parameter combinations, a stable dark soliton or dark pulse can form in the cavity. Meanwhile, the existence region of a single dark pulse increases with the frequency detuning parameter. The soliton essence of the obtained field profile is proved through the good fitting results based on a modified expression of the general dark soliton solution. Moreover, two routes to a stable dark soliton are identified, namely, originating from an

optical shock wave or a locally broad dark pulse. We also observe that when a single dark pulse with a wide and oscillatory bottom is formed in the microcavity, the comb spectral profile is modulated and exhibits a shoulder like structure.

References

[1] Del'Haye P, Schliesser A, Arcizet O, Wilken T, Holzwarth R and Kippenberg T J 2007 *Nature* **450** 1214
[2] Kippenberg T J, Holzwarth R and Diddams S A 2011 *Science* **332** 555
[3] Razzari L, Duchesne D, Ferrera M, Morandotti R, Chu S, Little B E and Moss D J 2010 *Nat. Photonics* **4** 41
[4] Wang T, Yang X, Liu X F, Lei F C, Gao M, Hu Y Q and Long G L 2015 *Acta Phys. Sin.* **64** 164212 (in Chinese)
[5] Jung H, Xiong C, Fong K Y, Zhang X F and Tang H X 2013 *Opt. Lett.* **38** 2810
[6] Okawachi Y, Saha K, Levy J S, Wen Y H, Lipson M and Gaeta A L 2011 *Opt. Lett.* **36** 3398
[7] Lei X, Bian D D and Chen S W 2016 *Chin. Phys. B* **25** 114214
[8] Grudinin I S, Yu N and Maleki L 2009 *Opt. Lett.* **34** 878
[9] Liang W, Savchenkov A A, Matsko A B, Ilchenko V S, Seidel D and Maleki L 2011 *Opt. Lett.* **36** 2290
[10] Savchenkov A A, Matsko A B, Ilchenko V S, Solomatine I, Seidel D and Maleki L 2008 *Phys. Rev. Lett.* **101** 093902
[11] Del'Haye P, Herr T, Gavartin E, Gorodetsky M L, Holzwarth R and Kippenberg T J 2011 *Phys. Rev. Lett.* **107** 063901
[12] Hugi A, Villares G, Blaser S, Liu H C and Faist J 2012 *Nature* **492** 229
[13] Griffith A G, Lau R K W, Cardenas J, Okawachi Y, Mohanty A, Fain R, Lee Y H D, Yu M, Phare C T, Poitras C B, Gaeta A L and Lipson M 2015 *Nat. Commun.* **6** 1
[14] Wang C Y, Herr T, Del'Haye P, Schliesser A, Holzwarth R, Hänsch T W, Picqué N and Kippenberg T J 2011 *Proceedings of the Quantum Electronics and Laser Science Conference*, May 1–6, 2011, Baltimore, Maryland, United States, p. 1
[15] Lecaplain C, Galy C J, Lucas E, Jost J D and Kippenberg T J 2015 *Proceedings of CLEO*, May 10–15, 2015, San Jose, California United States, p. S78
[16] Savchenkov A A, Ilchenko V S, Teodoro F Di, Belden P M, Lotshaw T W, Matsko A B and Maleki L 2015 *Opt. Lett.* **40** 3468
[17] Saha K, Okawachi Y, Levy J S, Lau R K W, Luke K, Foster M A, Lipson M, and Gaeta A L 2012 *Opt. Express* **20** 26935
[18] Herr T, Brasch V, Jost J D, Wang C Y, Kondratiev N M, Gorodetsky M L and Kippenberg T J 2014 *Nat. Photon.* **8** 145
[19] Hansson T, Modotto D and Wabnitz S 2015 *Phys. Rev. A* **88** 023819
[20] Liang W, Savchenkov A A, Ilchenko V S, Eliyahu D, Seidel D, Matsko A B and Maleki L 2014 *Opt. Lett.* **39** 2920
[21] Xue X X, Xuan Y, Liu Y, Wang P H, Chen S, Wang J, Leaird D E, Qi M H and Weiner A M 2015 *Nat. Photon.* **9** 594
[22] Chembo Y K and Menyuk C R 2013 *Phys. Rev. A* **87** 053852
[23] Haelterman M, Trillo S and Wabnitz S 1992 *Opt. Commun.* **91** 401
[24] Coen S, Randle H G, Sylvestre T and Erkintalo M 2013 *Opt. Lett.* **38** 37
[25] Xu X, Hu X H, Feng Y, Liu Y S, Zhang W, Yang Z, Zhao W and Wang Y S 2016 *Chin. Phys. B* **25** 034208
[26] Godey C, Balakireva I V, Coillet A and Chembo Y K 2014 *Phys. Rev. A.* **89** 063814
[27] Little B E, Laine J P and Haus H A 1999 *J. Lightwave Technol.* **17** 704
[28] Schiller S 1993 *Appl. Opt.* **32** 2181
[29] Agrawal G P 2007 *Nonlinear Fiber Optics*, 4th ed. (San Diego: Academic) p. 140
[30] Malaguti S, Bellanca G and Trillo S 2014 *Opt. Lett.* **39** 2475
[31] Rivas P P, Gomila D, Knobloch E, Coen S and Gelens L 2016 *Opt. Lett.* **41** 2402
[32] Lobanov V E, Lihachev G, Kippenberg T J and Gorodetsky M L 2015 *Opt. Express* **23** 7713
[33] Rivas P P, Knobloch E, Gomila D and Gelens L 2016 *Phys. Rev. A* **93** 063839